for the As + N_3 reaction is somewhat unexpected since, because of the greater spin–orbit coupling in this case, paths nominally forbidden by spin or orbital angular momentum correlations may well be more active.

To the extent that such angular momentum constraints operate in this system, the reaction is driven to produce excited triplet or quintet states of AsN as noted above. From the appearance of the new visible system in AsN (Figure 3), and comparison with known transitions[13] in N_2, PN, and similar molecules, this system is tentatively identified as a transition from an excited triplet of AsN to the ground state. We note in particular the strong Franck–Condon shift with respect to the ground state, the fact that the bands are red degraded, the substantially smaller ω_e in the upper state, and the energy of the state (T_e) with respect to that of the first excited singlet ($^1\Pi$). A comparison of these parameters for states of N_2, PN, and AsN is shown in Table III. Since the new excited state of AsN is not the a$^3\Pi$ state, it seems likely that it is a$'^3\Sigma^+$, the analogue of the A$^3\Sigma_u{}^+$ state in N_2. We note that the triplet state of PN produced from P + N_3 was also tentatively identified as a$'^3\Sigma^+$, based in that case on the single-headed nature of the bands.

The intensity of the visible bands and the time profile of the emission suggest that the excited triplet in AsN has a radiative lifetime considerably shorter than that of the PN analogue, as expected from the greater spin–orbit coupling. From the risetime of the PN a$'^3\Sigma^+ \rightarrow$ X$^1\Sigma^+$ emission found in previous experiments,[3] the lifetime of PN(a$'$) was determined to be greater than 4 ms. This lifetime, which allows for facile quenching by collisions with other species present and the reactor walls, accounted for the low intensity of these PN bands relative to the intensity of the PN A($^1\Pi$) $\rightarrow$ X($^1\Sigma^+$) system. In the present experiments, the rise of the AsN visible emission was mixing limited (suggesting $\tau \leq$ 1 ms), and the intensity of the visible emission was roughly equivalent to that of the AsN A($^1\Pi$) $\rightarrow$ X($^1\Sigma^+$) bands.

Summary and Conclusions

A new excited electronic state of AsN has been observed in chemiluminescence from the As + N_3 reaction. The state lies lower in energy than the known A($^1\Pi$) or a($^3\Pi$) states of AsN and radiates to the ground state in the visible region. The visible emission has spectroscopic characteristics which suggest that the excited state is a triplet metastable, likely the analogue of the $^3\Sigma^+$ excited states in PN and N_2.

Because of the larger spin–orbit coupling in AsN, it is not expected that angular momentum constraints are as strong in As + N_3 as in the analogous P + N_3 and N + N_3 reactions. Indeed, chemiluminescence from the reaction suggests the production of the A$^1\Pi$ state and possibly the a$^3\Pi$ state as well as the new excited triplet. The rate constant determined for the As + N_3 reaction indicates a trend in which $k(\mathrm{N+N_3}) > k(\mathrm{P+N_3}) > k(\mathrm{As+N_3})$.

Acknowledgment. This work was supported by the University of California, Los Alamos National Laboratory, under Subcontract 9X-25-X1451-1.

Infrared Spectra of O-Atom–PH_3 Reaction Products Trapped in Solid Argon

Robert Withnall and Lester Andrews*

Chemistry Department, University of Virginia, Charlottesville, Virginia 22901 *(Received: November 17, 1987; In Final Form: February 9, 1988)*

Argon/phosphine samples have been reacted with O atoms from a discharge, and the products trapped in solid argon for infrared spectroscopic analysis. Studies with isotopic precursors, stepwise photolysis, and sample annealing have made possible spectroscopic identification of PO, HPO, PO_2, PO_3, HOPO, P_2O_5, H_2PO, and HPOH, the last five for the first time. The PO_3 species appears to have D_{3h} symmetry from the isotopic out-of-plane bending mode absorption. Molecular P_2O_5 is formed on diffusion and reaction of PO_2 and PO_3. The major phosphine–oxygen atom reaction product H_2PO photoisomerizes to HPOH.

Introduction

There have been few experimental studies of simple oxides and oxyhydrides of phosphorus. Matrix codeposition of an Ar/PH_3 sample with Ar/O_2 passed through a microwave discharge produced PO and HPO, which were observed in the infrared and ultraviolet, as well as other unidentified products.[1] A recent study of the phosphine–ozone complex photolysis[2] gave infrared spectroscopic evidence for the novel H_3PO and H_2POH isomeric species as well as phosphonic acid ($(HO)_2HPO$) and HPO. The HOOPO, $HP(O_2)O$, and metaphosphoric acid ($HOPO_2$) molecules were also produced as secondary photolysis products in this latter matrix study.[3] In view of considerable current interest in reactions of phosphorus compounds and oxygen in general[4-7] and PO_2 in particular,[8-10] further infrared investigation of Ar/PH_3 samples codeposited at low temperature with Ar/O_2 samples passed through a microwave discharge has been conducted. This work verifies observations of PO and HPO from the previous study[1] as well as providing new infrared spectroscopic evidence for additional oxides and oxyhydrides of phosphorus.

Experimental Section

The cryogenic refrigeration system and vacuum vessel have been described previously.[11] PH_3 (Matheson) was used directly, and PD_3 was prepared by the reaction of D_2O with calcium phosphide.[2] Normal isotopic O_2 (Matheson, extra dry), and 55% and 98% ^{18}O-enriched samples (Yeda, Israel) were used from lecture bottles as received.

The first series of experiments studied the infrared spectra of products of the codeposition of Ar/PH_3 = 200 samples with Ar/O_2 = 50 samples flowing through a $^1/_4$-in. o.d. quartz tube in a microwave discharge *with the discharge plasma extending beyond*

---

[1] (a) Lazilliere, M.; Jacox, M. E. *NBS Spec. Publ.* **1978**, *No. 561*. (b) Larzilliere, M.; Jacox, M. E. *J. Mol. Spectrosc.* **1980**, *79*, 132.

[2] Withnall, R.; Hawkins, M.; Andrews, L. *J. Phys. Chem.* **1986**, *90*, 575.

[3] Withnall, R.; Andrews, L. *J. Phys. Chem.* **1987**, *91*, 784.

[4] Lohr, L. L. *J. Phys. Chem.* **1984**, *88*, 5569.

[5] Hamilton, P. A.; Murrells, T. P. *J. Chem. Soc., Faraday Trans. 2* **1985**, *81*, 1531.

[6] Stief, L. J.; Payne, W. A.; Nava, D. F. *J. Chem. Phys.* **1987**, *87*, 2112.

[7] Hamilton, P. A.; Murrells, T. P. *J. Phys. Chem.* **1986**, *90*, 182.

[8] Verma, R. D.; McCarthy, C. F. *Can. J. Phys.* **1983**, *61*, 1149.

[9] Kawaguchi, K.; Saito, S.; Hirota, E.; Ohashi, N. *J. Chem. Phys.* **1985**, *82*, 4893.

[10] Hamilton, P. A. *J. Chem. Phys.* **1987**, *86*, 33.

[11] Andrews, L. *J. Chem. Phys.* **1971**, *54*, 4935. Kelsall, B. J.; Andrews, L. *J. Phys. Chem.* **1981**, *85*, 1288.

0022-3654/88/2092-4610$01.50/0

the end of the tube toward the cold window. The microwave discharge was sustained by a diathermy (Burdick MW 200, 375 W) operating at 70–80% power in a standard Evenson–Broida cavity. Infrared spectra were recorded on a Nicolet 7199 FTIR spectrometer at 0.24 cm^{-1} resolution in the 4000–400-cm^{-1} range. Samples were irradiated for 20 min with a BH-6 high-pressure mercury arc lamp (1000 W, Illumination Ind., Inc.) in combination with a 10-cm water filter, which exposed the samples to 220–1000-nm radiation, and a further infrared spectrum was taken.

The second series of experiments examined infrared spectra of the products of the codeposition of $Ar/PH_3 = 200$ samples with $Ar/O_2 = 50$ samples passed through a low (20–30%) power microwave discharge *with the discharge plasma extending only to within 5 ± 1 cm of the end of the tube.* Samples were irradiated for 20-min intervals at progressively shorter wavelengths with the BH-6 high-pressure mercury arc lamp in combination with Corning glass and 10-cm water filters, which exposed the samples to the following wavelength ranges: A, 380–1000 nm; B, 290–1000 nm; full arc, 220–1000 nm. Infrared spectra were recorded on a Perkin-Elmer 983 spectrophotometer in the 4000–180-cm^{-1} range.

Results. Extended Discharge

The first series of experiments passed Ar/O_2 mixtures through *an extended* microwave discharge and codeposited this stream with Ar/PH_3. The infrared spectra exhibited weak PH_3 absorptions at 994 and 2340 cm^{-1}, which showed that *precursor was mostly destroyed by direct vacuum ultraviolet photolysis and by reaction with oxygen.* Product absorptions are shown in Figure 1 and listed in Table I; the product bands reveal several familiar species. Bands at 703.1, 1039.0, and 2109.0 cm^{-1} are assigned to ozone, and absorptions at 1101.0, 1388.5, and 3412.3 cm^{-1} are due to the hydroperoxyl free radical, HO_2, on the basis of comparison with earlier matrix spectra.[12,13] Sharp weak bands were identified at 804.0 and 759.3 cm^{-1} in $^{16}O_2$ and $^{18}O_2$ experiments, respectively, which are due to the isolated ozonide anion in solid argon.[14] In addition these bands became an isotopic sextet in $^{16,18}O_2$ experiments, and they were destroyed on full arc photolysis as befits an isolated anion with a low threshold for photodetachment.

Several phosphorus-containing products have been reported previously. The band at 1218.3 cm^{-1}, which red-shifted 45.2 cm^{-1} to 1173.1 cm^{-1} with ^{18}O and showed no deuterium shift, has already been identified as PO diatomic.[1] The absorption at 1187.2 cm^{-1}, which shifted to 1142.9 cm^{-1} with ^{18}O and 1185.3 cm^{-1} with deuterium, has been assigned to the HPO triatomic;[1,3] bands at 2098 and 998 cm^{-1} also belong to HPO.[1,3] Absorptions at 428.4, 445.7, 504.6, 908.4, 1185.3, 1445.6, and 3575.2 cm^{-1} have the appropriate relative intensities and isotopic shifts for metaphosphoric acid, $HOPO_2$ (labeled M in Figure 1).[3] Also, a weak doublet of bands in the P–O stretching region at 794.4 and 797.0 cm^{-1}, which shifted to 766.1 and 769.3 cm^{-1} with ^{18}O, can be assigned to phosphinous acid, PH_2OH.[3] The band at 1370.6 cm^{-1} shifted to 1329.7 cm^{-1} with ^{18}O and showed a small deuterium shift to 1369.2 cm^{-1}. Furthermore, with isotopically scrambled $^{16,18}O$, it gave rise to a 1:2:1:1:2:1 doublet of triplets. The foregoing data indicate that the 1370.6-cm^{-1} band is due to a phosphoryl (P=O) stretch in a species that contains two other equivalent oxygen atoms as well as hydrogen. This is consistent with assignment of the 1370.6-cm^{-1} band to the $HP(O_2)O$ species, which was recently been produced from photolysis of the PH_3–O_3 complex.[3] In addition, bands for six new products were present on codeposition of Ar/PH_3 and discharged Ar/O_2 samples. Some of the diagnostic bands will be described for different isotopic precursors.

TABLE I: Product Absorptions (cm^{-1}) Appearing in the First Series of Experiments on 12 K Codeposition of Ar/PH_3 = 200 Samples with Microwave-Discharged Ar/O_2 = 50 Samples

$PH_3/^{16}O_2$	$PH_3/^{18}O_2$	$PD_3/^{16}O_2$	$PD_3/^{18}O_2$	ident
406.0	405.1	303	302	**6**
424.5				?
428.4	419.5	435.2	425.2	$HOPO_2$
435.2	420.9		420.9	**2**
445.7	424.7	444.1	424.5	$HOPO_2$
446.7	425.7	445.0		
447.3	426.3	445.7		
458.8	441.7	456.2	439.3	Y
459.9	442.7	457.3	440.3	Y
479.5	459.2	479.5	459.2	**4**
480.3	470.0	480.3	470.0	**2**
504.6	501.6			$HOPO_2$
517.4	513.5			**3**
523.9	520.3			
529.0	525.8			
703.1	663.6	703.1	663.6	O_3
735.1	703.1			**4**
794.4	766.1			H_2POH
797.0	769.3			
804.0	759.3			O_3^-
817.7	788.1			**6**
841.5	810.0			**3**
848.0	816.8			
908.4	866.4	914.0	867.2	$HOPO_2$
955.7	955.3	710.5	710.5	**6**
1039.0	983.0	1039.0	983.0	O_3
1057.6	1047.3			?
1101.0	1039.8	1020		HO_2
		1137.7	1096.4	**5**
1147.7		1141.7	1100.4	
1151.7	1120.3	1143.8	1102.0	
1153.1	1122.2	1147.3	1105.8	
1152.5	1111.8	1152.5	1111.8	P_xO_y
1158.2	1105.5	1158.2	1105.5	**4**
1187.2	1142.9	1185.3	1141.1	HPO
1192.2	1146.8	1190.7	1143.9	$HOPO_2$[a]
1216.7	1171.5	1216.7	1171.5	PO–H_2
1218.3	1173.1	1218.3	1173.1	PO
1249.3	1204.8	1249.8	1204.8	**3**
1252.6	1207.7	1253.0	1207.8	
1253.5	1208.8	1254.5	1209.7	
1264.8	1226.4	1264.8	1226.4	P_xO_y
1266.0	1227.6	1266.0	1227.6	P_xO_y
1273.3	1234.5	1273.3	1234.5	**2**
1313.2	1312.7	1313.7	1312.7	X
1314.0	1313.5	1314.2	1313.5	X
1319.1	1280.2	1319.1	1280.2	**1**
1325.4	1286.1	1325.4	1286.1	
1370.6	1329.7	1369.2	1327.4	$HP(O_2)O$
1388.5	1379.5	1020.0	998.8	HO_2
1445.6	1405.3	1444.2	1402.9	$HOPO_2$[a]
1473.2	1431.3	1473.2	1431.3	**4**
1536.0	1450.0	1536.0	1450.0	O_2–X
2273.7	2276.5	1648.2	1647.5	**5**
2279.4		1658.6	1658.6	H_2POH
3412.3	3399.9	2529.6	2513.9	HO_2
3547.8	3537.0	2618.0	2602.3	**3**
3550.7	3540.6	2620.4	2604.6	
3555.1	3544.5	2623.4	2608.1	
3575.2	3564.8	2639.1	2623.3	$HOPO_2$[a]

[a] Shifted slightly from values reported in ref 3 owing to a different matrix environment.

PH_3 + ^{16}O. A triplet of bands for species **3** appeared at 3547.8, 3550.7, and 3555.1 cm^{-1} in the O–H stretching region. A band belonging to **5** appeared at 2273.7 cm^{-1} in the P–H stretching region. In the phosphoryl stretching region bands appeared at 1473.2 (**4**), 1319.1 with a weaker satellite at 1325.4 (**1**), 1249.3, 1252.6, and 1253.3 (**3**), 1158.2 cm^{-1} (**4**), and a site-split triplet at 1147.7, 1151.7 and 1153.1 cm^{-1} (**5**). A **3** doublet appeared at 841.6 and 848.2 cm^{-1} in the P–O stretching region. Finally in the phosphorus–oxygen deformation region split bands appeared at 517.4, 523.9, and 529.0 (**3**), 480.3 (**2**), 479.5 (**4**), 458.8 with a weaker satellite at 459.9 (Y) and 406.0 cm^{-1} (**6**). A product band appeared at 1536.1 cm^{-1}, in a region where new bands were not expected.

---

(12) Andrews, L.; Spiker, R. C., Jr. *J. Phys. Chem.* **1972**, *76*, 3208.

(13) Jacox, M. E.; Milligan, D. E. *J. Mol. Spectrosc.* **1972**, *42*, 495. Smith, D. W.; Andrews, L. *J. Chem. Phys.* **1974**, *60*, 81.

(14) Andrews, L.; Ault, B. S.; Grzybowski, J. M.; Allen, R. O. *J. Chem. Phys.* **1975**, *62*, 2461. Spiker, R. C.; Andrews, L. *J. Chem. Phys.* **1973**, *59*, 1851.

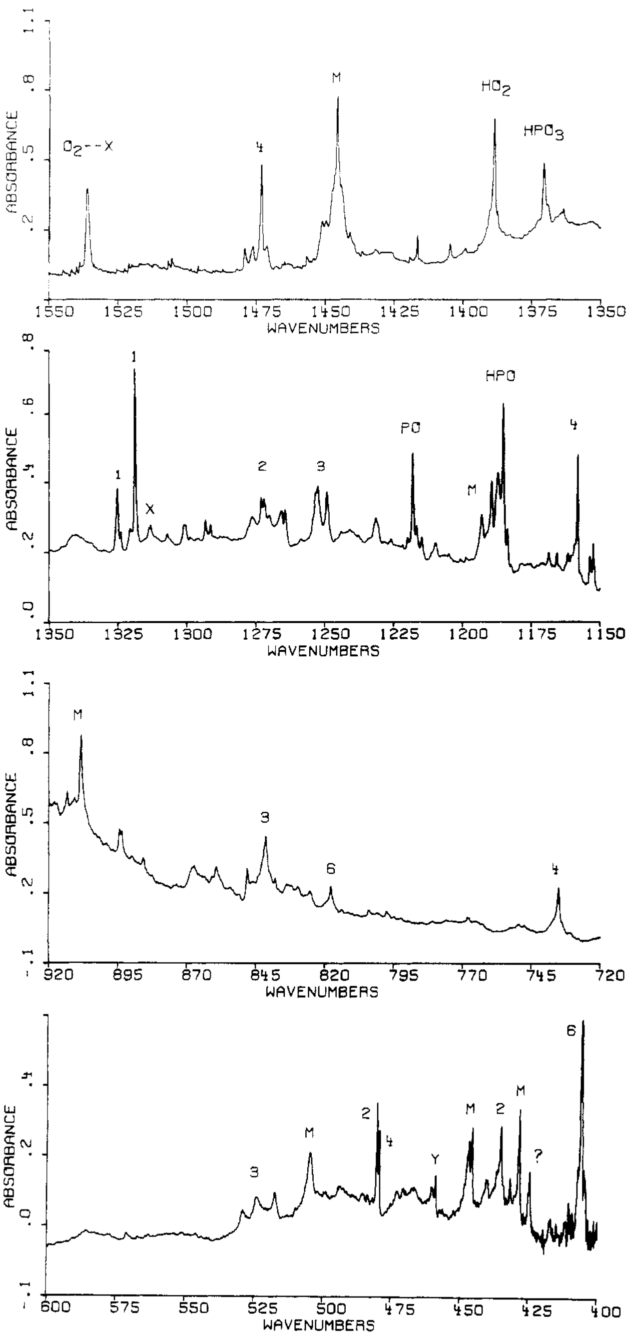

Figure 1. Infrared spectra of Ar/PH_3 = 200/1 sample codeposited at 12 K with Ar/O_2 = 50/1 mixture passed through extended microwave discharge.

PH_3 + ^{18}O. The major product bands were displaced upon ^{18}O substitution. The **3** triplet in the O–H stretching region shifted 10.5 ± 0.3 cm^{-1} to 3537.0, 3540.6, and 3544.5 cm^{-1} with ^{18}O. The **5** band at 2273.7 cm^{-1} was blue-shifted to 2276.5 cm^{-1}. The **4** band at 1473.2 cm^{-1} was red-shifted 41.9 cm^{-1} with ^{18}O to 1431.3 cm^{-1}. The sharp band at 1319.1 (**1**) was red-shifted 38.9 cm^{-1} to 1280.2 cm^{-1} with ^{18}O. The **3** triplet of bands at 1249.3, 1252.6, and 1253.3 cm^{-1} was red-shifted 44.7 ± 0.2 cm^{-1} to 1204.8, 1207.7, and 1208.8 cm^{-1}, respectively. The band at 1158.2 cm^{-1} (**4**) was red-shifted 52.7 cm^{-1} to 1105.5 cm^{-1}. The **5** bands at 1152.2 and 1153.9 cm^{-1} were red-shifted 31.1 and 30.9 cm^{-1} to 1121.1 and 1123.0 cm^{-1}, respectively. The **3** doublet at 841.5 and 848.2 cm^{-1} shifted 31.5 cm^{-1} to 810.0 and 816.8 cm^{-1}. In the phosphorus–oxygen deformation region, the **3** triplet shifted 3.6 ± 0.4 cm^{-1} to 513.5, 520.3, and 525.8 cm^{-1}, respectively. The **2** band at 480.3 cm^{-1} shifted 10.3 cm^{-1}, and the band at 479.5 cm^{-1} (**4**) shifted 20.3 cm^{-1}. The band at 459.9 cm^{-1} (Y) shifted 17.2 cm^{-1} to 442.7 cm^{-1}, and the **6** band at 406.0 cm^{-1} showed a small ^{18}O shift to 405.1 cm^{-1}. Finally the band at 1536.0 cm^{-1} showed a very large (86.0 cm^{-1}) shift to 1450.0 cm^{-1}.

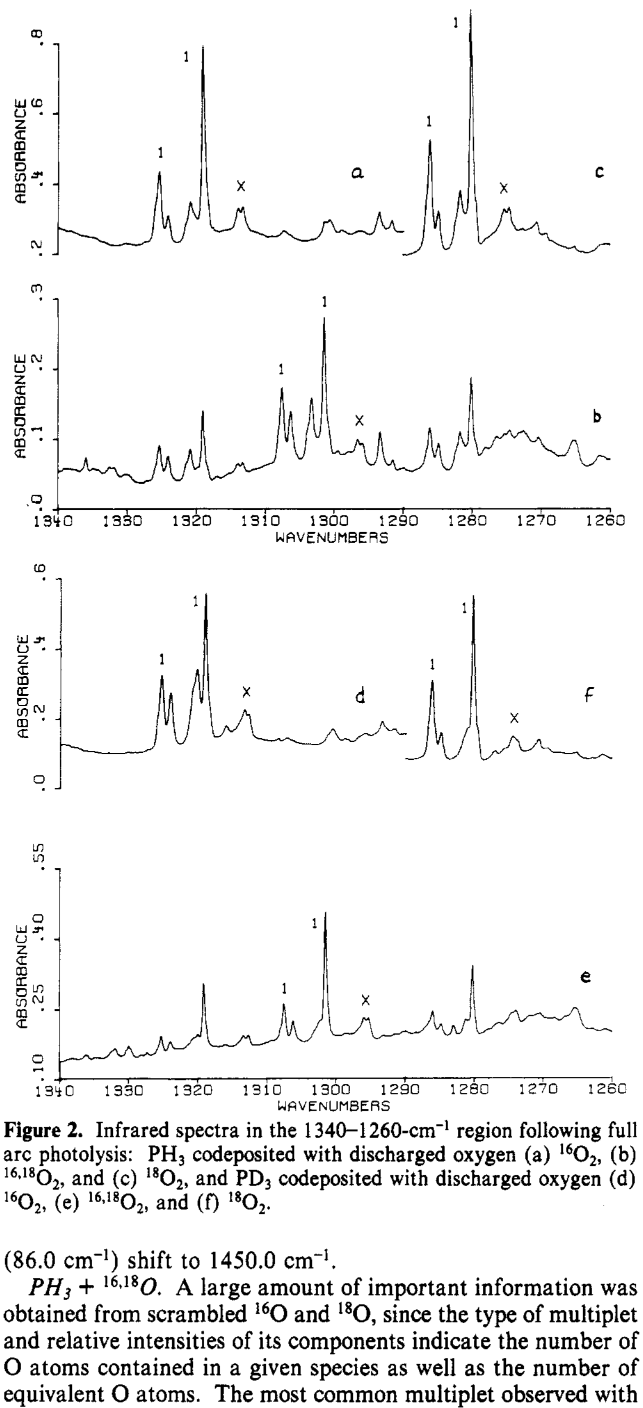

Figure 2. Infrared spectra in the 1340–1260-cm^{-1} region following full arc photolysis: PH_3 codeposited with discharged oxygen (a) $^{16}O_2$, (b) $^{16,18}O_2$, and (c) $^{18}O_2$, and PD_3 codeposited with discharged oxygen (d) $^{16}O_2$, (e) $^{16,18}O_2$, and (f) $^{18}O_2$.

PH_3 + $^{16,18}O$. A large amount of important information was obtained from scrambled ^{16}O and ^{18}O, since the type of multiplet and relative intensities of its components indicate the number of O atoms contained in a given species as well as the number of equivalent O atoms. The most common multiplet observed with ^{16}O and ^{18}O was a doublet with equal intensity components centered on the pure ^{16}O and pure ^{18}O peak locations as can be seen from Table II, which lists components in each multiplet. Some of the more interesting multiplets are shown in Figures 2–4.

PD_3 + ^{16}O. Deuterium substitution shifted many of the bands, which are listed in Table I along with their ^{18}O counterparts. Absorptions belonging to species **1**, **2** and **4** showed no deuterium shift. In the O–D stretching region, the **3** triplet at 2618.0, 2620.4, and 2623.4 cm^{-1} exhibited an H/D ratio of 1.355 with its protonated counterpart. In the P–D stretching region the **5** band at 1648.2 cm^{-1} exhibited an H/D ratio of 1.380 with its protonated counterpart. In the phosphoryl stretching region, the **5** bands at 1152.2 and 1153.9 cm^{-1} each shifted 6.3 cm^{-1}. In the 400–500-cm^{-1} region, the band at 458.8 cm^{-1} showed a 2.6-cm^{-1} red shift to 456.2 cm^{-1} on deuteriation.

PH_xD_{3-x} (x = 0–3) + O. In a scrambled PH_xD_{3-x}/^{16}O experiment a triplet of site-split doublets appeared in the phosphoryl stretching region at 1153.9, 1152.2, 1147.6, 1145.9, 1144.0, and 1142.0 cm^{-1}. This species **5** triplet disappeared on full arc irradiation. In a scrambled PH_xD_{3-x}/^{18}O experiment the components

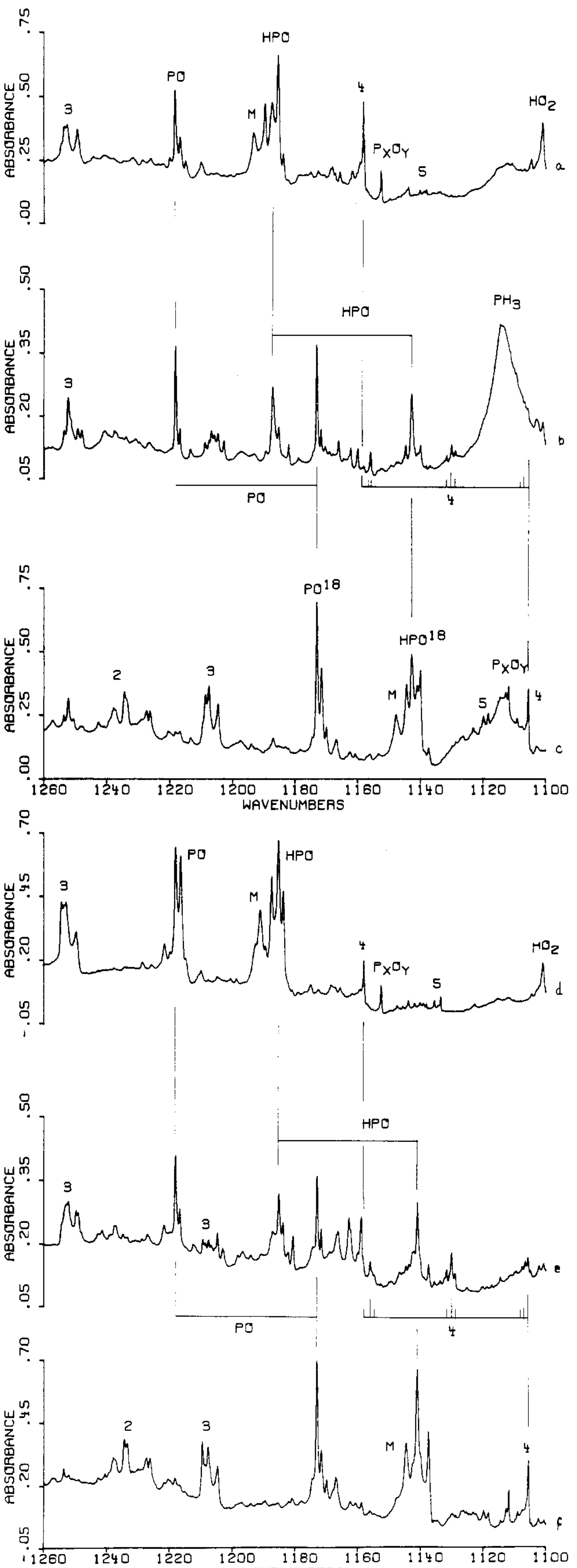

Figure 3. Infrared spectra in the 1260–1100-cm^{-1} region: PH_3 codeposited with discharged oxygen (a) $^{16}O_2$, (b) $^{16,18}O_2$, and (c) ^{18}O, and PD_3 codeposited with discharged oxygen (d) $^{16}O_2$, (e) $^{16,18}O_2$, and (f) $^{18}O_2$.

of the triplet of site-split doublets appeared at 1123.0, 1121.0, 1106.2, 1104.6, 1102.4, and 1100.6 cm^{-1} as shown in Figure 5.

Warming. On warming the matrix samples to 26 K for 5 min, species **2** bands and the 1325.4-cm^{-1} band, which is a satellite of the stronger species **1** band at 1319.1 cm^{-1}, decreased in intensity by 50%. There was no observed change in intensity for any of the other bands. On warming the matrix samples to 30 K for 10 min, bands belonging to species **2** disappeared, and the 1325.4-cm^{-1}

TABLE II: Oxygen Isotopic Product Absorptions (cm^{-1}) Observed in $^{16,18}O_2$ Discharge Experiments with PH_3 in Solid Argon

all ^{16}O	mixed $^{16,18}O$	all ^{18}O	ident
458.8	450.3	441.7	Y
459.8	451.4	442.7	Y
480.3	476.9, 473.4	470.0	PO_3
517.4	unresolved intermediate components	513.9	HOPO
523.9	unresolved intermediate component	520.3	HOPO
529.0	unresolved intermediate components	525.1	HOPO
794.6		766.3	H_2POH
797.6		769.3	H_2POH
841.5	839.8, 813.3	810.0	HOPO
848.2	846.4, 818.3	816.8	HOPO
1152.2		1121.1	H_2PO
1153.9		1123.0	H_2PO
1158.2	1156.0, 1155.38 1131.7, 1130.1, 1128.9, 1107.3, 1106.6	1105.5	P_2O_5
1185.3	1182.1, 1166.2, 1162.3, 1160.1, 1155.9, 1144.7	1140.0	$HOPO_2$
1187.2		1142.9	HPO
1216.7		1171.6	PO–H_2
1218.3		1173.1	PO
1249.3	1248.0, 1203.1	1205.0	HOPO
1252.6	1250.9, 1205.9	1207.7	HOPO
1253.5	1206.8	1208.8	HOPO
1313.2	1295.8	1274.6	X
1314.0	1296.6	1275.4	X
1319.1	1301.4	1280.2	PO_2
1325.4	1307.5	1286.1	PO_2
1370.6	1368.9, 1366.9, 1332.6, 1331.9	1329.7	HPO_3
1445.7	1442.2, 1429.48 1428.6, 1425.6, 1425.0, 1405.8	1405.4	$HOPO_2$
1473.2	1454.3, 1453.4, 1452.6	1431.3	P_2O_5
1536.0	1493.4	1450.0	O_2–X
3548.1		3537.1	HOPO
3551.0		3540.2	HOPO
3555.4		3544.8	HOPO
3575.8		3565.0	$HOPO_2$

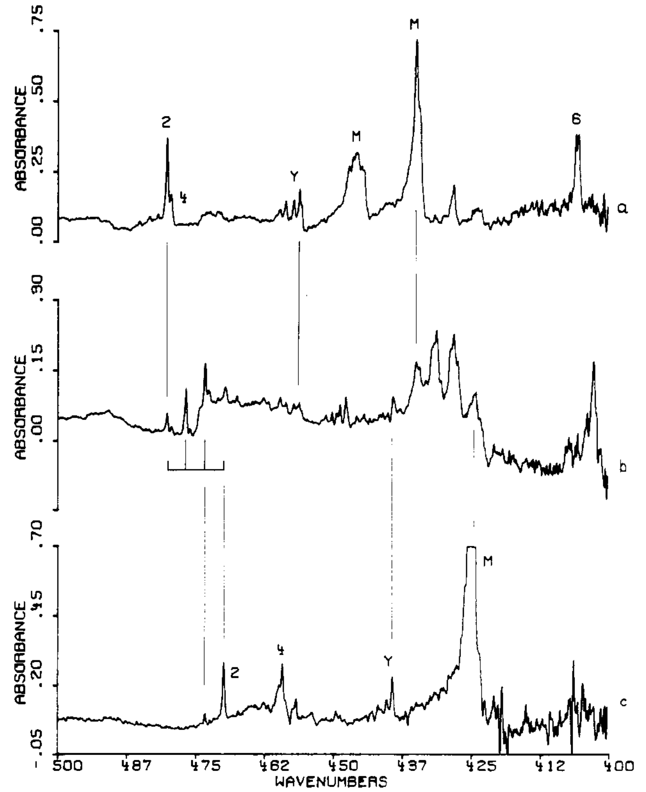

Figure 4. Infrared spectra in the 500–400-cm^{-1} region for PD_3 codeposited with discharged oxygen: (a) $^{16}O_2$, (b) $^{16,18}O_2$, and (c) $^{18}O_2$.

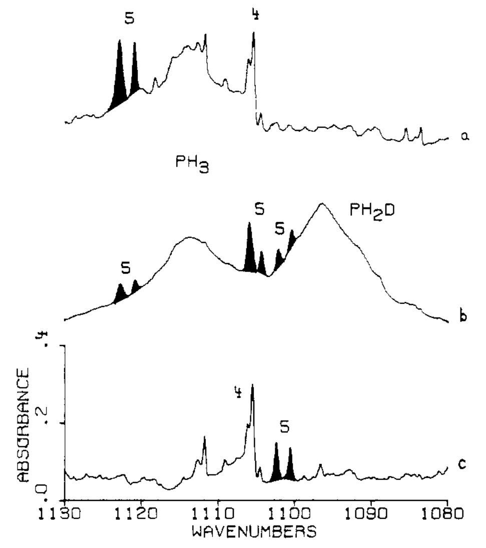

Figure 5. Infrared spectra in the 1130–1080-cm^{-1} region for phosphine codeposited with discharged $^{18}O_2$: (a) PH_3 and high-power discharge, (b) PH_xD_{3-x} mixture and low-power discharge to minimize higher oxide species **4**, and (c) PD_3 and high-power discharge.

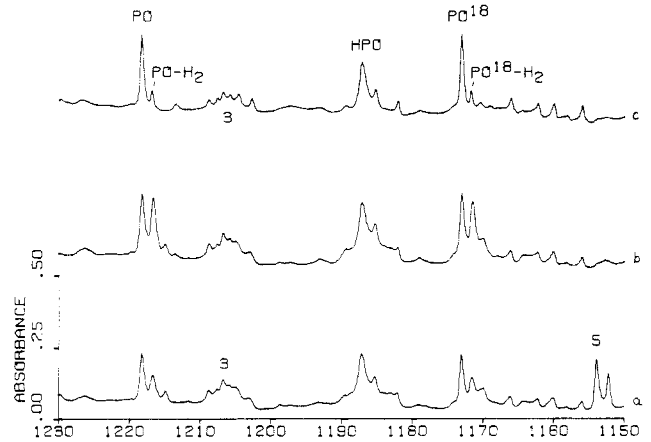

Figure 6. Infrared spectra in the 1230–1150-cm^{-1} region: (a) PH_3 codeposited at 12 K with discharged $^{16,18}O_2$, (b) after 220–1000-nm photolysis for 30 min, and (c) after warming to 30 K for 10 min and recooling to 12 K.

band decreased in intensity by 70%. The PO satellite band at 1216.7 cm^{-1} also disappeared, and the 1218.3 cm^{-1} isolated PO band grew (see Figure 6). The group of bands at 479.5, 735.1, 1158.2, and 1473.2 cm^{-1} (species **4**) increased, and the other product bands decreased slightly in intensity. In addition, a blue emission was observed first at 18–22 K, which became very strong at 32 K.

Results. Mild Discharge

The second series of experiments discharged Ar/O_2 in *milder, shorter* plasmas. Unlike the first series of experiments, infrared spectra of codeposited Ar/PH_3 exhibited strong PH_3 absorptions at 994, 1114, 2340, and 2345 cm^{-1}. This indicates that PH_3 was not photolyzed with vacuum ultraviolet light to the same extent as in the first series of experiments and that *oxygen atom reactions with PH_3 itself are dominant here.* The product spectrum is shown in Figure 7, and band positions and absorbances after deposition and three filtered irradiations are listed in Table III. Bands are separated into the same six groups based on irradiation and sample warming: group 1, produced on deposition, slight increase with irradiation A and B, increased 2× on full arc irradiation; group 2, produced on deposition, no change with A, B, and full arc irradiations, disappeared on warming to 30 K; group 3, produced on deposition, no change with A, B, and full arc irradiations; group 4, weak on deposition, stable on photolysis, increased on sample annealing; group 5, produced on deposition, decreased on irradiation A, disappeared on irradiation B; group 6, present on deposition, increased 4× with irradiation A, decreased with B and full arc irradiations. These changes are illustrated in Figure 7 for the 800–1350-cm^{-1} spectral region; other regions exhibited analogous behavior. The PO band at 1218.3 cm^{-1} and its satellite at 1216.7 cm^{-1} were both present on deposition and increased in intensity throughout the irradiation sequence.

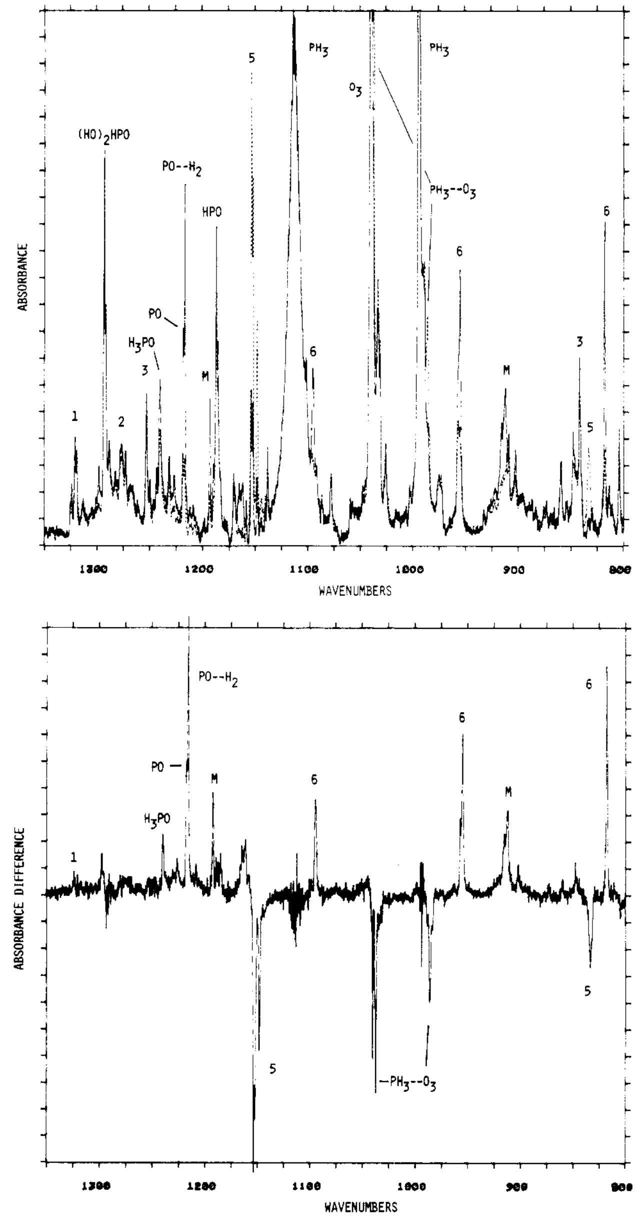

Figure 7. Infrared spectra in the 1350–800-cm^{-1} region for PH_3 codeposited with O_2 passed through low-power discharge: top, dashed spectrum after deposition, solid spectrum after 380–1000-nm photolysis for 20 min; bottom, difference between dashed and solid traces from top, bands above base line grew on photolysis, and bands below base line decreased on photolysis.

Discussion

Identification and vibrational assignments of the product species will be given. Products **1–4** will be identified first; these were prevalent in the first series of experiments, which involved almost complete vacuum ultraviolet photolysis and reaction of PH_3.

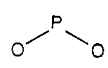
1

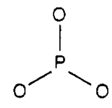
2

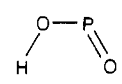
3

*PO_2 (Species **1**).* The band at 1319.1 cm^{-1} with a satellite at 1325.4 cm^{-1} is attributed to PO_2 triatomic as discussed below. PO_2

TABLE III: Absorbances of Product Bands (cm^{-1}) Appearing in the Second Series of Experiments on 12 K Codeposition of Ar/PH_3 = 200 Samples with Discharged Ar/O_2 = 50 Samples and after Irradiation A, Irradiation B, and Full Arc Irradiation

abs,[a] cm^{-1}	codepstn	A	B	full arc	ident
406.3	0.02	0.08	0.06	0.04	**6**
428.4	0.02	0.04	0.04	0.05	$HOPO_2$
435.2	0.01	0.01	0.01	0.01	**2**
447.3	0.02	0.06	0.06	0.07	$HOPO_2$
458.8	0.06	0.06	0.06	0.06	Y
459.9	0.03	0.03	0.03	0.03	Y
479.5	0.02	0.02	0.02	0.02	**4**
480.3	0.01	0.01	0.01	0.01	**2**
504.6	0.01	0.03	0.03	0.03	$HOPO_2$
517.4	0.08	0.08	0.08	0.08	**3**
703.8	0.09	0.09	0.09	0.07	O_3
735.1	0.02	0.02	0.02	0.02	**4**
747.4	0.14	0.14	0.14	0.12	
780.7	0.08	0.08	0.08	0.06	
794.4	0.04	0.04	0.04	0.07	PH_2OH
797.0	0.08	0.17	0.17	0.19	PH_2OH
817.7	0.06	0.23	0.18	0.12	**6**
833.1	0.08	0.02			**5**
841.6	0.17	0.17	0.17	0.17	**3**
848.2	0.02	0.04	0.04	0.04	**3**
908.4	0.03	0.20	0.24		$HOPO_2$
955.7	0.1	0.32	0.32	0.30	**6**
986	0.2				$PH_3–O_3$
1037	0.4				$PH_3–O_3$
1076	0.09	0.09	0.09	0.09	?
1094.4	0.04 (sh)	0.16	0.13	0.08	**6**
1101.0	0.04	0.04	0.04	0.04	HO_2
1147.7	0.15	0.02			**5**
1151.7	0.35	0.08			**5**
1153.1	0.46	0.10			**5**
1158.2	0.02	0.02	0.02	0.02	**4**
1187	0.32	0.32	0.32	0.32	HPO
1192.2	0.01	0.07	0.07	0.09	$HOPO_2$
1216.7	0.07	0.32	0.38	0.44	$PO–H_2$
1218.3	0.07	0.17	0.19	0.25	PO
1240.2	0.10	0.17	0.19	0.21	H_3PO
1252.6	0.10	0.11	0.11	0.11	**3**
1294	0.34	0.34	0.34	0.28	$(HO)_2HPO$
1319.1	0.08	0.10	0.10	0.20	**1**
1325.4	0.02	0.03	0.03	0.06	**1**
1370.6	0.04	0.04	0.04		$HP(O_2)O$
1388.5	0.17	0.17	0.17	0.17	HO_2
1445.6	0.20	0.27	0.33		$HOPO_2$
1473.2	0.03	0.03	0.03	0.03	**4**
2273.8	0.24	0.03			**5**
2279.4	0.03	0.06	0.06	0.06	PH_2OH
3412.3	0.04	0.04	0.04	0.04	HO_2
3550.7	0.07	0.07	0.07	0.07	**3**
3575.2	0.03	0.16	0.16	0.19	$HOPO_2$

[a] Absorbances given for most intense band in site-split multiplet.

has recently been detected in gas-phase discharges by using far-infrared laser magnetic resonance and microwave spectroscopies;[9] from the observed rotational constants PO_2 is a C_{2v} molecule with r(P–O) = 1.467 Å and ∠(OPO) = 135.3°. The laser-induced fluorescence spectrum and radiative lifetime of PO_2 have also been reported recently;[8] the subject was generated by reaction of atomic oxygen with P_4, PH_3, PCl_3, and PBr_3. The method of production of PO_2 in the present study is identical—the reaction of discharged oxygen with PH_3 (or P_4).[15]

The 1319-cm^{-1} band was tentatively assigned to $(PO)_2$ in the earlier matrix study, although the PO_2 possibility was not ruled out.[1b] The $(PO)_2$ dimer species is expected to have a similar structure to the cis-planar nitric oxide dimer, $(NO)_2$,[16] and the symmetric and antisymmetric PO stretches in $(PO)_2$ should have similar ^{18}O shifts to a pure PO oscillator in this frequency region (49.4 cm^{-1}). The band at 1319.1 cm^{-1} has a considerably lower ^{18}O shift of 38.9 cm^{-1}, which rules out the $(PO)_2$ assignment. It is better assigned to the antisymmetric P–O stretch of a species with two identical P–O oscillators having a common phosphorus atom. Taking the valence angle of PO_2 triatomic from the microwave study,[9] the ^{18}O isotopic shift can be calculated from the G matrix elements for the antisymmetric stretches of $P^{16}O_2$ and $P^{18}O_2$. This predicts that the 1319.1-cm^{-1} band will be shifted 39.5 cm^{-1}, in good agreement with the observed shift of 38.9 cm^{-1}. There is no error introduced into this calculation through coupling with other modes since the antisymmetric stretch is alone in the B_2 symmetry class in this C_{2v} molecule. The calculated frequency is 0.05% lower than that observed, which is the magnitude expected for anharmonicity. Furthermore, the 1:2:1 relative intensity of the triplet with central component at 1301.4 cm^{-1} using $^{16,18}O_2$ in the discharge requires a species with two equivalent oxygen atoms. The fact that no deuterium shift was observed on the oxygen isotopic triplet bands at 1319.1, 1301.4, and 1280.2 cm^{-1} strongly suggests that this species does not contain any hydrogen (see Figure 2). Similar experiments with P_4 (from white phosphorus) and discharged Ar/O_2 = 50/1 samples gave a sharp band at 1319.1 cm^{-1} with the same ^{18}O shift and the same triplet with mixed $^{16,18}O$ as that observed in PH_3/O atom experiments.[15]

TABLE IV: Isotopic Fundamentals (cm^{-1}) Observed for *cis*-HOPO in Solid Argon

		$H^{16}OP^{16}O$		$H^{18}OP^{18}O$	$D^{16}OP^{16}O$	$D^{18}OP^{18}O$
ν(O–H)	a′	3550.7	(3560)[a]	3540.6	2620.4	2604.6
ν(P=O)	a′	1252.6	(1270)	1207.7	1253.0	1207.8
δ(P–O–H)	a′		(955)			
ν(P–O)	a′	841.5	(844)	810.0		
$\delta(PO_2)$	a′		(393)			
τ(OPOH)	a″	523.9	(546)	520.3		

[a] Frequencies predicted for *cis*-HOPO by ab initio calculations,[23] which have been scaled by a factor of 0.89; scaled *trans*-HOPO predictions are 3618, 1291, 944, 823, 406, and 441 cm^{-1}.

The presence in these experiments of a weak PO diatomic band at 1218.3 cm^{-1}, shifting to 1173.1 cm^{-1} with ^{18}O, indicates that single P atoms were produced and reacted with discharged oxygen. On account of the foregoing it is chemically reasonable for the 1319.1-cm^{-1} band produced with both PH_3 (and P_4)[15] to belong to a PO_2 species. The presence of weak isolated O_3^- bands requires consideration of PO_2^-, which absorbs at 1207 cm^{-1} in solid KCl,[17] but the anion identification is unlikely on the basis of observations for NO_2^- in KCl (1275 cm^{-1}) and solid argon (1244 cm^{-1}).[18] The latter comparison predicts isolated PO_2^- at 1180 ± 20 cm^{-1} in solid argon. Furthermore, the 1319.1-cm^{-1} band grows on photolysis and the O_3^- anion is destroyed, which rules out the PO_2^- possibility. Finally, the observation of the near-UV electronic absorption[8] of PO_2 in solid argon in similar experiments in this laboratory strongly supports the stabilization of PO_2 in these experiments.

Taking the gas-phase value for the symmetric PO stretch of $P^{16}O_2$ (1117 ± 20 cm^{-1})[10] and the matrix antisymmetric PO stretching frequency of PO_2 and neglecting the bend, the diagonal and off-diagonal PO stretching force constants can be obtained from a (2 × 2) GF matrix calculation. This gives values of 9.46 × 10^2 and 0.76 × 10^2 N m^{-1} for F(PO) and F(PO, PO), respectively, which compares well with the F(PO) value of 9.8 × 10^2 N m^{-1} for $ClPO$[19] and 9.24 × 10^2 N m^{-1} for PO diatomic. Finally, the bond-stretching force constants for PO and PO_2 follow the trend in bond lengths (r for PO is 1.476 Å).[20]

The symmetric PO_2 stretch expected in the 1100-cm^{-1} region was not observed. It is quite possible that it comes under the broad PH_3 band centered at 1114 cm^{-1}. However since bands due to the symmetric stretches of $P^{18}O_2$ and $P^{16}O^{18}O$ were not observed either, it seems very likely that the symmetric PO_2 stretch is very

---

(15) Andrews, L.; Withnall, R. *J. Am. Chem. Soc.*, in press.

(16) Kukolich, S. G. *J. Mol. Spectrosc.* **1983**, *98*, 80.

(17) Hunter, S. J.; Hipps, K. W.; Francis, A. H. *Chem. Phys.* **1979**, *39*, 209.

(18) Kato, R.; Rolfe, J. *J. Chem. Phys.* **1967**, *47*, 1901. Milligan, D. E.; Jacox, M. E. *J. Chem. Phys.* **1971**, *55*, 3404.

(19) Binnewies, M.; Lakenbrink, M.; Schnockel, H. *Z. Anorg. Allg. Chem.* **1983**, *497*, 7.

(20) Ngo, T. A.; DaPaz, M.; Coquart, B.; Couet, C. *Can. J. Phys.* **1974**, *52*, 154.

much weaker than the antisymmetric PO_2 stretch. Assuming zero coupling with the bending vibration, the ratio of intensities of the antisymmetric and symmetric stretches of the PO_2 triatomic is given approximately by the relationship[21]

$$I_a/I_s = ((\partial\mu/\partial Q_3)/(\partial\mu/\partial Q_1))^2 = \tan^2(\alpha/2) = 6$$

where $\partial\mu/\partial Q$ is the dipole moment change in the normal mode and α is the PO_2 valence angle. Of course this assumes no electronic rehybridization during bond stretching. This assumption may not hold since the analogous NO_2 triatomic has a similar valence angle (134°),[22] and I_a is at least 2 orders of magnitude greater than I_s.

The bend of PO_2 has been estimated at 377 cm^{-1} from the centrifugal distortion constants[9] and measured at 387 ± 20 cm^{-1} from the laser-induced fluorescence spectrum.[10] Unfortunately the region below 400 cm^{-1} was not accessible in the FTIR experiments, but the PO_2 bend was not observed in the 300–400-cm^{-1} region with the grating instrument probably because of low intensity.

PO_3 (Species 2). The diagnostic band for species **2** appeared at 480.3 cm^{-1}. With mixed $^{16,18}O$ this band gave a quartet with components at 470.0, 473.4, 476.9, and 480.3 cm^{-1} and 1:3:3:1 relative intensities (see Figure 4), which clearly indicates three equivalent oxygen atoms. Furthermore, none of these bands showed a deuterium shift, and species **2** does not appear to contain hydrogen. For the above reasons, species **2** is identified by PO_3. Ab initio calculations predict a $^2A_2'$ ground-state σ-radical of D_{3h} symmetry with a bond length of 1.455 Å. A $^2E''$ π-radical state of D_{3h} symmetry is predicted to be low-lying and to give rise to $^2B_1$ and $^2A_2$ Jahn–Teller branches both of C_{2v} symmetry.[23]

The D_{3h} structure has A_1', A_2'', $2E'$ vibrational modes with the totally symmetric stretch (A_1') not infrared active. The stretching and bending E' vibrational modes are both predicted to be Jahn–Teller active.[23] The band at 480.3 cm^{-1} can be assigned to the out-of-plane wag (A_2'') of a PO_3 species of D_{3h} symmetry. From the diagonal G matrix elements for the wag, the band at 480.3 cm^{-1} is calculated to shift to 476.8 cm^{-1} in $P^{16}O^{16}O^{18}O$ (observed for 476.9 cm^{-1}), to 473.3 cm^{-1} in $P^{16}O^{18}O^{18}O$ (observed = 473.4 cm^{-1}), and to 469.7 cm^{-1} in $P^{18}O_3$ (observed = 470.0 cm^{-1}). The excellent agreement between calculated and observed isotopic shifts of the wag indicates that ground-state PO_3 is indeed of D_{3h} symmetry as predicted by theory.[23] Infrared diode laser spectroscopy of the analogous NO_3 radical indicated that the $^2A_2'$ ground state is also of D_{3h} symmetry.[24]

The band at 1273.3 cm^{-1}, which shifts to 1234.5 cm^{-1} with ^{18}O and shows no deuterium shift, is assigned to the antisymmetric stretch (E') of PO_3. The observed ^{18}O shift of 38.8 cm^{-1} (somewhat less than the shift of 47 cm^{-1} of a pure PO oscillator in this region) is in reasonable agreement with the value of 40.6 cm^{-1} calculated from the diagonal G matrix elements. Unfortunately no multiplet was seen with mixed $^{16,18}O$, presumably because it was too weak to be observed. Furthermore the band at 435.2 cm^{-1}, which shifts 14.3 cm^{-1} with ^{18}O and has no deuterium shift, is tentatively assigned to the deformation mode (E') of PO_3. It was predicted at 439 cm^{-1} by scaling the 493-cm^{-1} theoretical frequency.[23]

Finally, the bands attributed to PO_3 disappeared on warming to 30 K for 10 min with an accompanying growth in bands of species **4**.

HOPO (Species 3). Bands belonging to species **3** listed in Table IV are assigned to *cis*-HOPO as is now discussed. The band at 3551.0 cm^{-1} shifting 10.8 cm^{-1} with ^{18}O is clearly an O–H stretch. The band at 1252.6 cm^{-1} shifting 44.9 cm^{-1} with ^{18}O is due to a phosphorus–oxygen double bond stretch. The P=O stretch of the analogous ClPO molecule in solid argon has been observed at 1257.7 cm^{-1} with an ^{18}O shift of 45.9 cm^{-1}.[19] With mixed $^{16,18}O$, the site-split triplet at 1249.3, 1242.6, and 1253.5 cm^{-1} gives rise to a multiplet shown in Figure 3. This multiplet appears to consist of a doublet of doublets for the site-split triplet. One component is at 1205.0, 1207.7, and 1208.8 cm^{-1} due to pure $H^{18}OP^{18}O$, and a further component, presumably due to $H^{16}OP^{18}O$, is red-shifted approximately 2 cm^{-1} from this at 1203.1, 1205.9, and 1206.8 cm^{-1}. The bands at 1249, 1250.9, 1252.4, and 1253.6 cm^{-1} are almost certainly due to the site-split triplet of pure $H^{16}OP^{16}O$ at 1249.3, 1252.6, and 1253.5 cm^{-1} unresolved from a further site-split triplet due to $H^{18}OP^{16}O$. A similar multiplet was obtained with PD_3 and mixed $^{16,18}O$. Two components of a doublet of doublets appeared at 1204.8, 1207.8, and 1209.7 and 1203.4, 1206.8, and 1208.8 cm^{-1} due to $D^{18}OP^{18}O$ and $D^{16}OP^{18}O$, respectively. The components due to $D^{16}OP^{16}O$ and $D^{18}OP^{16}O$ are also unresolved. This multiplet provides evidence for the second O atom, which weakly perturbs the P=O stretching frequency on ^{18}O substitution. It suggests that the O–P=O angle is close to 90°, giving a small G matrix element connecting the two stretching modes. Two facts suggest that the P=O stretch of the $H^{18}OP^{18}O$ and $H^{16}OP^{18}O$ isotopes may be in Fermi resonance with the O–P=O bend and P–O stretch combination. First, a shift of the P=O stretch was observed in going from $H^{18}OP^{18}O$ to $H^{16}OP^{18}O$, whereas the P=O stretches of $H^{16}OP^{16}O$ and $H^{18}OP^{16}O$ could not be resolved. Second, the P=O stretch of $H^{16}OP^{16}O$ and $H^{18}OP^{16}O$ could not be resolved. Second, the P=O stretch of $H^{16}OP^{18}O$ was observed 2 cm^{-1} to the red of the P=O stretch of $H^{18}OP^{18}O$, whereas it would be expected to come to slightly higher energy on account of the mass effect. If the O–P=O bend of $H^{16}OP^{16}O$ comes at 393 cm^{-1} as predicted by theory (see Table IV), the the $\nu_4 + \nu_5$ combination is likely to come below ν_2 in $H^{18}OP^{18}O$ but above it in $H^{16}OP^{18}O$. A similar Fermi resonance may occur in $D^{18}OP^{18}O$ and $D^{16}OP^{18}O$.

TABLE V: Isotopic Fundamentals (cm^{-1}) Observed for the H_2PO Radical

	^{16}O, H	^{18}O, H	^{16}O, D	^{18}O, D
$\omega(PH_2)$	791.6	790.5	602.9	600.8
δ(HPO)	833.2	830.4	628.4	624.2
ν(PO)	1147.7		1137.7	1096.4
	1151.7	1120.3	1141.7	1102.0
	1153.1	1122.2	1147.3	1105.8
ν(PH)	2273.8	2276.5	1648.2	1647.5
	2275.7			
2ν(PO)	2287.2			
	2293.4			
	2296.4			

Similarly in the P–O stretching region the site-split doublet at 841.5 and 848.0 cm^{-1}, which shifted to 810.0 and 816.9 cm^{-1} with ^{18}O, was split into a quartet of site-split doublets with mixed $^{16,18}O$. The P–O stretch appears as a quartet with mixed $^{16,18}O$ as the result of a weak perturbation by the P=O stretch.

Vibrational frequencies have been calculated for both *cis*- and *trans*-HOPO isomers,[23] and these are listed in Table IV. As can be seen from the table, the agreement between the theoretical frequencies of *cis*-HOPO and the observed values is very good. In particular there is good agreement between the theoretical value of 546 cm^{-1} for ν_6 of *cis*-HOPO and the observed value of 523.9 cm^{-1}. The agreement between the theoretical frequencies of *trans*-HOPO and the observed values is not quite as good. Therefore, on this basis, the observed bands are assigned to the *cis*-HOPO isomer. This is consistent with the theoretical prediction that the cis isomer is lower (17 kJ mol^{-1}) in energy than the trans isomer. No ultraviolet or infrared photoisomerization of HOPO was observed, unlike the analogous HONO molecule for which photoinduced isomerization has been reported.[25]

P_2O_5 (Species 4). The following evidence identifies species **4** as molecular P_2O_5. The band at 1473.2 cm^{-1}, which shifted 41.9 cm^{-1} to 1431.3 cm^{-1} with ^{18}O, is clearly due to a phosphoryl stretch.

---

(21) Burdett, J. K.; Poliakoff, M.; Turner, J. J.; Dubost, H. *Adv. Infrared Raman Spectrosc.* **1976**, *2*, 1.

(22) Bowman, W. C.; DeLucia, F. C. *J. Chem. Phys.* **1982**, *77*, 92.

(23) Lohr, L. L.; Boehm, R. C. *J. Phys. Chem.* **1987**, *91*, 3203.

(24) Ishiwata, T.; Tanaka, I.; Kawaguchi, K.; Hirota, E. *J. Chem. Phys.* **1985**, *82*, 2196.

(25) Baldeschwieler, J. D.; Pimentel, G. C. *J. Chem. Phys.* **1960**, *33*, 1008. Hall, R. T.; Pimentel, G. C. *J. Chem. Phys.* **1963**, *38*, 1889.

Similarly the band at 1158.2 cm^{-1}, which shifted 52.7 cm^{-1} to 1105.5 cm^{-1} with ^{18}O, is also due to a phosphoryl stretch. Assuming an O–P–O bond angle of approximately 135° by analogy with PO_2,[9] $ClPO_2$,[26] and $HOPO_2$,[3] the ^{18}O shifts suggest that the bands at 1158.2 and 1473.2 cm^{-1} are due to symmetric and antisymmetric $-PO_2$ stretching modes, respectively. Analogous motions for $HOPO_2$ were observed at 1193 and 1451 cm^{-1}, respectively,[3] and for $ClPO_2$ at 1148 and 1448 cm^{-1}, respectively.[26] With mixed $^{16,18}O$, the band at 1158.2 cm^{-1} gave rise to a triplet of triplets with relative intensities 1:2:1:2:4:2:1:2:1 (see Figure 3 and Table II). This multiplet suggests that the band at 1158.2 cm^{-1} is due to a phosphoryl stretch involving two equivalent oxygen atoms perturbed by another group with two equivalent oxygen atoms. Mixed $^{16,18}O$ splits the band at 1473.2 cm^{-1} into a multiplet based on a triplet model, with the middle component of the "triplet" split into a further triplet. Components of this multiplet are located at 1431.3, 1452.6, 1453.4, 1454.3, and 1473.2 cm^{-1} with relative intensities of 2:1:1:2:2. There are no close satellites for the 1473.2 or 1431.3 cm^{-1} pure isotopic components, which seems to indicate that the antisymmetric stretching frequency of a $-P^{16}O_2$ or $-P^{18}O_2$ group of P_2O_5 is not perturbed by the two oxygen atoms of the other $-PO_2$ group. However, the central component for the $-P^{16}O^{18}O$ isotopic species of lower symmetry is split into a secondary triplet owing to a slight mixing of the "symmetric" and "antisymmetric" stretching modes. This is presumably because the net motion of the atoms of the $-PO_2$ group in the antisymmetric stretch is perpendicular to the P–O bond of the P–O–P skeleton, resulting in no mechanical coupling between the antisymmetric stretches of the $-PO_2$ groups through the skeletal P–O–P stretching modes. A similar situation arises for the antisymmetric $-PO_2$ stretch of $HOPO_2$, which was not perturbed by the third oxygen atom.[3] Of course, in the symmetric $-PO_2$ stretch of P_2O_5, the $-PO_2$ groups can couple through the P–O–P skeleton.

The remaining two bands that were observed for P_2O_5 appeared at 735.1 and 479.5 cm^{-1}. The band at 735.1 cm^{-1} is almost certainly due to a stretching mode of the P–O–P skeleton since symmetric P–O–P stretches fall in the 650–800-cm^{-1} region and antisymmetric P–O–P stretches appear in the 850–1060-cm^{-1} region for a number of compounds.[27] With a value of 128° for the P–O–P angle,[27] the symmetric P–O–P stretch is predicted to shift 21.8 cm^{-1} and the antisymmetric counterpart 32.1 cm^{-1} from the G matrix elements for these motions. The excellent agreement with the 32.1-cm^{-1} calculated and the 32.0-cm^{-1} observed shift and the expected greater intensity for the antisymmetric skeletal motion suggests this assignment for the 735.1-cm^{-1} band. This P–O–P mode is crucial for the identification of P_2O_5 since the central oxygen atom did not manifest itself in the mixed isotopic multiplets. The band at 479.5 cm^{-1}, which has an ^{18}O shift of 20.3 cm^{-1}, is very likely due to a $-PO_2$ deformation mode. No multiplets were observed with mixed $^{16,18}O$ for either the 735.1- or 479.5-cm^{-1} bands, which is in keeping with high isotopic dilution for vibrational modes involving a large number of oxygen atoms.

Two possible structures for P_2O_5 are **4a** and **4b**, both of which have a bent central P–O–P group and are of C_{2v} symmetry. It was inferred above from the mixed $^{16,18}O$ multiplet that there was no detectable coupling between the $-PO_2$ groups in the antisymmetric stretching mode at 1473.2 cm^{-1}. Since only one band appeared in the 1473.2-cm^{-1} region, it seems likely that the antisymmetric stretches of the $-PO_2$ groups are accidentally degenerate. It has been suggested that the antisymmetric N–O stretches of the two nitro groups of the analogous N_2O_5 molecule, in the gas phase, are also accidentally degenerate.[28] This accidental degeneracy indicates that the two $-PO_2$ groups are likely equivalent, as is the case in both proposed structures. It has also been previously mentioned that the triplet of triplets, which replaced the 1158.2-cm^{-1} band with mixed $^{16,18}O$, suggested that the two oxygen atoms in both $-PO_2$ groups are equivalent. This favors the saddle structure **4b**, since the two oxygen atoms in the $-PO_2$ groups of the planar **4a** are not equivalent.

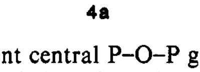

4a

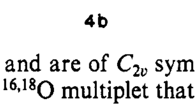

4b

In support of the above assignment, bands at 1157 and 1473 cm^{-1} in the matrix investigation of $ClPO_2$ were tentatively assigned to hydrolysis products.[26] These bands are almost certainly due to the same species as the bands at 1158.2 and 1473.2 cm^{-1}, which are assigned here to P_2O_5 in solid argon. The band at 1473.2 cm^{-1} is the highest frequency observed for a $-PO_2$ antisymmetric stretch, and this is consistent with a very high electronegativity for the $-PO_3$ substituent. The electron affinity of the PO_3 radical has recently been predicted to be 5.4 ± 0.2 eV by ab initio calculation.[23] P_2O_5 is most likely formed here from combination of PO_2 and PO_3 radicals as a growth of P_2O_5 bands on annealing is clearly accompanied by a decrease of bands due to PO_3. Finally, experiments in this laboratory using YAG laser evaporation, decomposition, and matrix trapping of P_4O_{10} from a pressed disk have produced strong absorptions at 1408, 1026, 768, and 577 cm^{-1} for P_4O_{10}, sharp weak 1473-, 1158-, and 736-cm^{-1} bands for P_2O_5, and the sharp 1319-cm^{-1} absorption assigned here to PO_2. The production of the P_2O_5 and PO_2 bands from laser ablation supports their identification from O + PH_3 reactions.

The milder discharge conditions of the second series of experiments favored species **5** and **6**. Vibrational assignments and analyses of species **5** and **6** are now given, and reaction mechanisms are proposed to account for their formation.

H_2PO (Species 5). Although recent experimental investigations provide mass spectroscopic evidence for H_2PO radical as the principal product of the reaction between PH_3 and $O(^3P)$,[5,6] it has not hitherto been observed by optical means. Bands that decreased on irradiation A and disappeared on irradiation B can be assigned to the H_2PO radical (species **5**; see Table V).

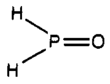

5

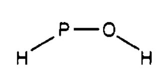

6

The site-split triplet at 1147.7, 1151.7, and 1153.1 cm^{-1}, which was red-shifted 31 cm^{-1} with ^{18}O (see Table I), is clearly due to a phosphorus–oxygen stretch. On deuteriation it was red-shifted by 6 cm^{-1}, and the ^{18}O red shift of fully deuteriated D_2PO was 41 cm^{-1}. The reason that the ^{18}O shift of the P=O stretch of H_2PO (31 cm^{-1}) is considerably less than that of D_2PO (41 cm^{-1}) is most likely due to coupling of the P=O stretch with the H–P–H bend, which is expected in the 1100-cm^{-1} region by analogy with the PH_2 triatomic.[1a] On deuteriation the H–P–H bend shifts into the 800-cm^{-1} region and interacts much less strongly with the P=O stretch. With $^{16,18}O_2$ the triplet at 1147.7, 1151.7, and 1153.1 cm^{-1} gives rise to a doublet of site-split triplets centered on the frequency locations of the triplets present with pure ^{16}O and pure ^{18}O, as expected, since H_2PO contains a single O atom. With scrambled PH_xD_{3-x} (x = 0–3), and ^{18}O, the P=O stretch gives the strongest two bands present with $PH_3/^{18}O$ and the strongest two bands present with $PD_3/^{18}O$ as well as two intermediate new bands at 1104.4 and 1106.2 cm^{-1} (black bands in Figure 5). This triplet of site-split bands provides evidence that H_2PO contains two equivalent H atoms. The band at 2274.8 cm^{-1} in the P–H stretching region shows an unusual blue-shift with ^{18}O to 2276.5 cm^{-1}. This is due to interaction of this P–H stretching mode with the overtone of the P=O stretch. The overtone of the P=O stretch of $H_2P^{16}O$ is observed as a weak, site-split triplet at 2287.2, 2293.4, and 2296.4 cm^{-1} to the blue of the P–H stretching band at 2274.8 cm^{-1}. The overtone of the PO stretch

---

(26) Ahlrichs, R.; Ehrhardt, C.; Lakenbrink, M.; Schunck, S.; Schnockel, H. *J. Am. Chem. Soc.* **1986**, *108*, 3596.

(27) Corbridge, D. E. C. *Top. Phosphorus Chem.* **1969**, *6*, 235–365.

(28) Hisatsune, I. C.; Devlin, J. P.; Wada, Y. *Spectrochim. Acta* **1962**, *18*, 1641.

of $H_2P^{18}O$ is unobserved, but it is expected to come approximately 10 cm^{-1} lower (anharmonicity correction) than 2244 cm^{-1} (=2 × 1122 cm^{-1}). This accounts for the 1.7-cm^{-1} blue-shift of the P–H stretching band of H_2PO, on ^{18}O substitution, since the overtone of the P=O stretch comes just above it in $H_2P^{16}O$ but below it in $H_2P^{18}O$. It seems more than likely that the band at 2274.8 cm^{-1} is due to the symmetric P–H stretch, since it will have the same symmetry as the overtone of the P=O stretch whether H_2PO is pyramidal or planar with C_{2v} symmetry.

The band at 833.2 cm^{-1}, which had an ^{18}O shift of 2.9 cm^{-1}, is assigned to the PH_2 rock of H_2PO as it comes in the same region as this mode in PH_2OH (848.1 cm^{-1}).[3] On deuteriation it shifted down to 628.4 cm^{-1} (H/D ratio 1.326), and the ^{18}O shift of the D_2PO band was 4.2 cm^{-1}. The 791.6- and 602.9-cm^{-1} bands of H_2PO and D_2PO had small ^{18}O shifts and are assigned to the PH_2 (PD_2) wag.

Structures have been predicted for both pyramidal and planar forms of H_2PO at the UHF level.[29] The P=O stretching frequency for H_2PO is substantially higher than that for H_2POH, which favors the planar form having the shorter P=O bond.

HPOH (*Species 6*). Bands belonging to species 6 were present on deposition, increased 4× with irradiation A at the expense of H_2PO, and decreased with B and full arc irradiation in favor of PO–H_2 complex and isolated PO. These bands (see Table VI) are assigned to the HPOH isomer. The band at 817.7 cm^{-1}, which shifts 29.6 cm^{-1} with ^{18}O down to 788.1 cm^{-1}, is clearly due to a P–O single bond stretch as it comes very close to the P–O stretch of H_2POH (797.1 cm^{-1}). The band at 1094.4 cm^{-1} is assigned to a P–O–H bend owing to the ^{18}O shift and by comparison to the P–O–H bend of H_2POH (1074.8 cm^{-1}).[3] The band at 406.3 cm^{-1} comes in the appropriate region for the torsion and has appropriate ^{18}O and deuterium shifts. The strong band at 955.7 cm^{-1} with a very small ^{18}O shift (0.4 cm^{-1}) and a large deuterium shift to 710.5 cm^{-1} can be assigned to the H–P–O bend since it comes close to the bend of HPO triatomic (998.0 cm^{-1}).[3] Unfortunately the O–H stretch was not detected due to insufficient signal in the high-frequency region, but the O–D stretch was observed at 2689.0 cm^{-1} (shifting 16.0 cm^{-1} with ^{18}O). No band appeared in the P–H stretching region appropriate for the P–H stretch of HPOH, probably on account of masking by other bands or weak intensity.

The optimized geometries and heats of formation of cis- and trans-planar isomers of HNOH, the nitrogen-containing analogue of HPOH, have been calculated by using the semiempirical molecular orbital method, MINDO/3.[30] The cis-planar isomer of HNOH was predicted to be 5.5 kcal mol^{-1} more stable than the trans-planar isomer from these calculations. Although similar calculations have not been performed for HPOH, cis-planar HPOH is likely more stable than its trans-planar isomer by analogy.

HPOH is formed by photoisomerization of H_2PO at wavelengths shorter than approximately 420 nm. Bands due to HPOH were diminished by radiation of shorter wavelengths than 290 nm. Photodissociation of HPOH was accompanied by growth of the band at 1216.7 cm^{-1}, which is almost certainly due to a complex of PO diatomic with H_2. Annealing to 30 K for 10 min almost completely destroyed this complex band with a concomitant growth in the nearby band at 1218.3 cm^{-1} due to isolated PO diatomic (see Figure 7).

Other Species. A weak doublet at 1313.2 and 1314.0 cm^{-1} (labeled X in Table I), which grew slightly on full arc photolysis and annealing, remains unidentified. It showed a 0.5-cm^{-1} red shift with deuterium and shifted 38.6 cm^{-1} with ^{18}O to 1274.6 and 1275.4 cm^{-1}. Furthermore, with mixed $^{16,18}O$, a 1:2:1 triplet of site-split doublets was observed. These bands of species X are almost certainly due to a $-PO_2$ antisymmetric stretch as they come in the same region as the band at 1319.1 cm^{-1}, assigned here to the antisymmetric stretch of PO_2 radical, and have a similar ^{18}O shift. It is possible that species X is PH_2PO_2, but the data do not allow a definitive identification.

TABLE VI: Isotopic Fundamentals (cm^{-1}) Observed for the HPOH Radical

	^{16}O, H	^{18}O, H	^{16}O, D	^{18}O, D
τ(HPOH)	406	405	303	302
ν(PO)	817.7	788.1	816.6	787.3
δ(HPO)	955.7	955.3	710.5	710.5
			820.2	813.9
δ(POH)	1094.4	1089.6	821.8	814.7
ν(OH)			2689.0	2673.0

The band at 458.8 cm^{-1} (labeled Y in Table I) was present on deposition, showed no change with full arc irradiation, and decreased by approximately 30% on annealing to 30 K for 10 min. Furthermore it did not appear to track with any other bands. With ^{18}O it shifted 17.1 cm^{-1} down to 441.7 cm^{-1}, which is an ^{18}O shift expected for a pure PO oscillator in this region or alternatively the shift expected for an O–P–O valence angle bend of a $-PO_2$ group having a bond angle of 90°. With mixed $^{16,18}O$, the band at 458.8 cm^{-1} gave rise to a 1:2:1 triplet with components at 441.7, 450.3, and 458.8 cm^{-1}, suggesting species Y contains two equivalent oxygen atoms. The middle component at 450.3 cm^{-1} came, to the nearest 0.1 cm^{-1}, midway between the pure ^{16}O and pure ^{18}O components. In view of this shift and appearance in the O–P–O deformation region, the band at 458.8 cm^{-1} is attributed to a valence angle bend of a $-PO_2$ group. With scrambled PH_xD_{3-x} (x = 0–3), bands appeared 458.8 and 456.3 cm^{-1}, the respective pure H and pure D band locations, indicating Y contains a single H atom. The foregoing suggests that species Y may be a pyramidal HPO_2 species with H–P–O and O–P–O bond angles close to 90°, approximately the same as the H–P–H bond angle of PH_3.[27] Such a species is likely to be a biradical with an unpaired electron density on each O atom. The O–P–O bend would involve a large charge redistribution and result in a strong infrared absorption. No other bands belonging to Y were observed, since they are presumably weaker. A pyramidal HPO_2 biradical species could be formed by reaction of ground-state O(^{3}P) with HPO.

The band at 1152.5 cm^{-1} and the doublet at 1264.8 and 1266.0 cm^{-1}, which showed no deuterium shifts, are attributed to separate phosphorus oxide species of general formula P_xO_y. The 1152.5-cm^{-1} band showed an ^{18}O shift of 40.7 cm^{-1} down to 1111.8 cm^{-1} and unfortunately had an indiscernible isotopic pattern with mixed $^{16,18}O$ on account of the isotopic dilution, and it is probably the symmetric PO_2 stretch in another species. The doublet at 1264.8 and 1266.0 cm^{-1} showed an ^{18}O shift of 38.4 cm^{-1} down to 1266.4 and 1227.6 cm^{-1}, and again the isotopic splittings appeared to be very small and unresolved. Although the species contributing the doublet at 1264.8 and 1266.0 cm^{-1} is unknown, a phosphorus oxide containing more than one P atom such as P_2O_3 is possible, especially since P_2O_5 has been identified here.

Finally, the band at 1536 cm^{-1} is clearly due to an O_2 complex on the basis of band position and isotopic behavior. This complex clearly involves a reactive molecule as discharge conditions were required. The lack of a deuterium shift, and observation of the 1536-cm^{-1} band in YAG experiments with P_4O_{10} and extended O_2 discharge experiments[15] with P_4 suggest a O_2–P_xO_y complex.

Mechanisms. The previous study of the 1216-Å photolysis of PH_3 during condensation in solid argon demonstrated the ease of formation of P_2.[1] Since 1216-Å radiation is far beyond the threshold for photolytic rupture of P–H bonds, it is likely that P atoms were liberated from PH_3. Likewise, under the intense vacuum ultraviolet radiation produced by the protruding Ar/O_2 discharge in the first series of experiments, P atoms are likely to play an important role in the chemical reactions. Scheme I is therefore suggested as a plausible set of reactions to account for the major products in the first series of experiments.

---

(29) Yabushita, S.; Gordon, M. S. *Chem. Phys. Lett.* **1985**, *117*, 321.

(30) Loew, G. H.; Berkowitz, D. S.; Chang, S. *Astrophys. J.* **1978**, *219*, 458.

SCHEME I

$$P(^4S) + P(^4S) \rightarrow P_2(^1\Sigma_g^+) \tag{1}$$

$$P(^4S) + O(^3P) \rightarrow PO(^2\Pi) \tag{2}$$

$$PO(^2\Pi) + O(^3P) \rightarrow PO_2(^2B_1) \tag{3}$$

$$PO_2(^2B_1) \rightarrow PO_2(^2A_1) + h\nu \tag{4}$$

$$P(^4S) + O_2(^3\Sigma_g^-) \rightarrow PO_2(^2A_1) \tag{5}$$

$$PO_2(^2A_1) + O(^3P) \rightarrow PO_3(^2A_2') \tag{6}$$

$$PO_2 + PO_3 \rightarrow P_2O_5 \tag{7}$$

$$PH(^3\Sigma) + O(^3P) \rightarrow HPO(^1A') \tag{8}$$

$$PH(^3\Sigma) + O_2(^3\Sigma_g^-) \rightarrow cis\text{-HOPO} \tag{9}$$

$$HPO(^1A') + O_2(^3\Sigma_g^-) + h\nu \rightarrow HOPO_2(^1A') \tag{10}$$

By contrast under the milder discharge conditions employed in the second series of experiments, reactions involving P atoms did not play such a major role. Instead, O-atom reactions with phosphorus hydrides were more prevalent in this set of experiments. Scheme II is proposed to explain the major products identified in the second series of experiments.

SCHEME II

$$PH_3 + O(^3P) \rightarrow H_2PO\ (\text{doublet}) + H(^2S) \tag{11}$$

$$H(^2S) + O_2(^3\Sigma) \rightarrow HO_2\ (\text{doublet}) \tag{12}$$

$$PH_2(^2S) + O(^3P) \rightarrow H_2PO\ (\text{doublet}) \tag{13}$$

$$H_2PO + h\nu\ (<420\text{ nm}) \rightarrow HPOH \tag{14}$$

$$HPOH + h\nu\ (<290\text{ nm}) \rightarrow PO\text{---}H_2 \tag{15}$$

$$PO\text{---}H_2 \xrightarrow{\text{annealing}} PO \tag{16}$$

$$H_2PO(\text{doublet}) + HO_2\ (\text{doublet}) \rightarrow (HO)_2HPO\ (\text{singlet}) \tag{17}$$

Formation of $PO_2(^2B_1)$ in reaction 3 has been previously suggested to explain the green chemiluminescence, (4), observed in gas-phase reactions of oxygen with a variety of phosphorus-containing compounds.[7] Also, PO_2 has very recently been observed in low-temperature matrices by electron spin resonance from the reaction of P atoms with molecular O_2 as in reaction 5 above.[31] The PO_2 radical can add an O atom, reaction 6, to give the PO_3 radical observed here for the first time. The formation of P_2O_5 in reaction 7 is analogous to the formation of N_2O_5 from NO_2 and NO_3. Reaction of atomic and molecular oxygen with PH to give HPO and *cis*-HOPO, respectively (reaction 8 and 9) presumably takes place with little or no activation energy at these low temperatures. Formation of *cis*-HOPO from reaction of PH and O_2 (reaction 9) is exactly analogous to the formation of nitrous acid, HONO, from the reaction of NH with O_2 in low-temperature matrices.[25] The synthesis of metaphosphoric acid, $HOPO_2$, in the photochemical reaction of HPO with O_2 (reaction 10) has previously been proposed in PH_3/O_3 photolysis studies.[3]

Formation of H_2PO in the second series of experiments occurs by reaction of ground-state oxygen atoms with either PH_3 (reaction (11) or PH_2 radicals (reaction 13). Reaction 11 is apparently fast in the gas phase, proceeding via an addition/decomposition mechanism,[5,6] and this same reaction is likely to occur during reagent condensation. Addition of $O(^3P)$ to PH_3 does not yield ground-state phosphine oxide as this reaction pathway is spin forbidden,[32] and the yield of H_3PO was substantially less in the present O-atom reaction experiments than from photolysis of the PH_3–O_3 complex.[3] However, $O(^3P)$ atoms probably add to PH_2 radicals to give H_2PO without an activation energy barrier, since calculations have indicated that, on the doublet surface, the analogous addition of O atoms to NH_2 should form H_2NO without an activation energy barrier.[33] On the other hand, there was no evidence for a low-temperature reaction of PH_2 radicals with O_2 in this work, and calculations have predicted that the analogous NH_2 radical does not form a very stable O_2 complex.[33] Finally, the formation of $(HO)_2HPO$ can be accounted for by the reaction of H_2PO and HO_2 radicals (reaction 15); these radicals could be produced in close proximity via reactions 11 and 12.

It has previously been pointed out that, since isolated[14] O_3^- is present in these discharge experiments, it is possible that phosphorus oxide anions are also produced.[1] However isolated anion absorptions are expected to decrease in intensity on full arc irradiation on account of electron detachment.[34] Even PO_2^- is expected to photodetach with full arc irradiation.[4] Only the bands due to O_3^- and those already assigned to H_2PO and HPOH neutrals showed this behavior. Furthermore, the infrared bands due to the PO_2 and PO_3 radicals, which have high electron affinities, show the same photolysis and warm-up behavior as structured electronic bands attributed to these species beginning at 300 and 695 nm.[35] Negatively charged PO_2^- and PO_3^- species are not expected to have electronic absorptions in these regions.

Conclusions

The reaction of discharge-produced O atoms and PH_3 molecules during condensation with excess argon forms and traps a number of phosphorus oxides and oxyhydrides. Many of these new species are in common with those from previous gas-phase and matrix experiments. The ν_3 fundamental of PO_2 has been assigned at 1319 cm^{-1}. The PO_3 molecule has been observed for the first time and characterized as a D_{3h} species from a 1:3:3:1 out-of-plane bending quartet absorption with $^{16,18}O$ reactions. The important HOPO intermediate has been identified by O–H, O–P, and P=O stretching modes. The association of PO_2 and PO_3 gives molecular P_2O_5, which has phosphoryl stretching modes near $HOPO_2$ values and a diagnostic P–O–P stretching fundamental at 735 cm^{-1}. The symmetric phosphoryl stretching mode exhibits a triplet of triplets with $^{16,18}O$ demonstrating two equivalent $-PO_2$ groups. The H_2PO radical formed by the direct reaction of PH_3 and O atoms photoisomerizes to the HPOH radical, which is characterized by different matrix infrared fundamentals. The matrix traps at least 10 intermediate species in the reaction of O atoms with PH_3 that often react further in the gas-phase discharge to give more stable or higher aggregate species.

Acknowledgment. We gratefully acknowledge support from NSF Grant CHE 85-16611 and helpful correspondence and original spectra from M. E. Jacox.

Registry No. PO, 14452-66-5; HPO, 13817-06-6; PO_2, 12164-97-5; PO_3, 12651-01-3; HOPO, 14097-15-5; P_2O_5, 1314-56-3; H_2PO, 97516-21-7; HPOH, 114996-56-4; O, 17778-80-2; PH_3, 7803-51-2; Ar, 7440-37-1; D_2, 7782-39-0; ^{18}O, 14797-71-8.

---

(31) Knight, L., private communication, 1987.

(32) Schmidt, M. W.; Gordon, M. S. *J. Am. Chem. Soc.* **1985**, *107*, 1922.

(33) Melius, C. F.; Binkley, J. S. *ACS Symp. Ser.* **1984**, *249*, 103.

(34) Andrews, L. *Annu. Rev. Phys. Chem.* **1979**, *30*, 79.

(35) Withnall, R.; McCluskey, M.; Andrews, L. *J. Phys. Chem.*, to be published.